



저작자표시 2.0 대한민국

이용자는 아래의 조건을 따르는 경우에 한하여 자유롭게

- 이 저작물을 복제, 배포, 전송, 전시, 공연 및 방송할 수 있습니다.
- 이차적 저작물을 작성할 수 있습니다.
- 이 저작물을 영리 목적으로 이용할 수 있습니다.

다음과 같은 조건을 따라야 합니다:



저작자표시. 귀하는 원저작자를 표시하여야 합니다.

- 귀하는, 이 저작물의 재이용이나 배포의 경우, 이 저작물에 적용된 이용허락조건을 명확하게 나타내어야 합니다.
- 저작권자로부터 별도의 허가를 받으면 이러한 조건들은 적용되지 않습니다.

저작권법에 따른 이용자의 권리는 위의 내용에 의하여 영향을 받지 않습니다.

이것은 [이용허락규약\(Legal Code\)](#)을 이해하기 쉽게 요약한 것입니다.

[Disclaimer](#) 

Master's Thesis

석사 학위논문

Validation of Grip Force Measurement Using Hand
Rehabilitation Robot for Impedance Control

Jihyuk Park (박 지 혁 朴 志 赫)

Department of Robotics Engineering

로봇공학전공

DGIST

Master's Thesis

석사 학위논문

Validation of Grip Force Measurement Using Hand
Rehabilitation Robot for Impedance Control

Jihyuk Park (박 지 혁 朴 志 赫)

Department of Robotics Engineering

로봇공학전공

DGIST

Validation of Grip Force Measurement Using Hand Rehabilitation Robot for Impedance Control

Advisor : Professor Pyung Hun Chang

Co-Advisor : Professor Sung Ho Jang

by

Ji Hyuk Park

Department of Robotics Engineering

DGIST

A thesis submitted to the faculty of DGIST in partial fulfillment of the requirements for the degree of Master of Science, in the Department of Robotics Engineering. The study was conducted in accordance with Code of Research Ethics

1. 9. 2015

Approved by

Professor Pyung Hun Chang (Signature)
(Advisor)

Professor Sung Ho Jang (Signature)
(Co-Advisor)

Validation of Grip Force Measurement Using Hand Rehabilitation Robot for Impedance Control

Ji Hyuk Park

Accepted in partial fulfillment of the requirements for the degree of Master of
Science.

12. 4. 2014

Head of Committee	<u>Prof. Pyung Hun Chang</u>	(인)
Committee Member	<u>Prof. Sung Ho Jang</u>	(인)
Committee Member	<u>Prof. Jong Hyun Kim</u>	(인)

MS/RT 박 지 혁. Jihyuk Park. Validation of grip force measurement using hand rehabilitation robot
201223006 for impedance control. Department of Robotics Engineering. 2014. 49p. Advisors Prof.
Chang, Pyung Hun, Prof. Co-Advisors Jang, Sung Ho.

ABSTRACT

Recently, a novel hand rehabilitation robot was developed in an authors' laboratory for the rehabilitation of patients with neurological disorders such as strokes. In terms of mechanism this robot has features not only to provide full grasping motion by using one motor but also to have finger length adjustment for various people. Although the robot has aforementioned advantages, for impedance control, force information sensed from F/T sensor is not validated yet. Since it is required to figure out the direct force of hand during grasping and opening motion, the reliability of force information needs to be confirmed for applying impedance control to our hand robot.

Using simulation tool, Autodesk ForceEffect™, force analysis of the hand robot is implemented. Under three different MCP angles such as 0°, 30°, and 60°, known force is applied at the end-point of the hand robot and torque at F/T sensor can be calculated considering gear ratio. Then, under same condition experiment is carried out. In this case, force is applied using digital dynamometer and torque is directly measured by F/T sensor.

As a result, at all cases except for MCP angle 0°, analysis and experiment result have highly linear relation ($R^2 = 0.9916, R^2 = 0.9917$, at MCP angle 30° and 60° respectively). By this relationship, fingertip force can be estimated approximately. Therefore, the foundation of impedance control is established and it leads to the expectation that the impedance control based hand robot will provide the therapy compliant to the patients more precisely, more comprehensively, and much safely.

Keywords: grip force, hand rehabilitation robot, impedance control,

List of Contents

Abstract	i
List of Contents	ii
List of Tables.....	iv
List of Figures.....	v

I . INTRODUCTION

1.1 Purpose of Research	1
1.2 Structure of Thesis	2

II . BACKGROUND

2.1 Stroke	3
2.2 Hand Joint Anatomy	4
2.3 Neurological Hand Impairment Following Stroke	5
2.4 Grip Force Measurement Tools.....	6
2.5 Impedance Control	7

III. METHODS AND ANALYSIS

3.1 Introduction to the Developed Hand Rehabilitation Robot	9
3.1.1 Hardware.....	9
3.1.2 Software.....	12
3.1.3 Kinematics and Mechanism of the Developed Hand Robot.....	15
3.1.3.1 Verification of Its Mobility by Grübler’s and Alizade’s Formula.....	15
3.2 Analysis of the Developed Hand Rehabilitation Robot	16
3.2.1 Introduction to Analysis Tool, Autodesk ForceEffect™.....	16
3.2.2 Force Analysis of the Hand Rehabilitation Robot using ForceEffect™	17
3.2.2.1 The Effect of Magnitude and Angle error of Applied Force	21

IV. EXPERIMENTS AND RESULTS

4.1 Verification of Torque Using Hand Robot with Applied Force by Digital Dynamometer	23
4.1.1 Experimental Setup and Tasks	23
4.1.2 Data Analysis	24
4.1.3 Experiment Results	25
4.1.4 Discussion	27
4.1.4.1 MCP Angle Deviation According to Magnitude of Applied Force	27
4.1.5 Results of Modified Analysis of the Hand Robot	29

V. CONCLUSION

5.1 Study Summary	33
5.2 Constraints	34
5.3 Future Directions	35

List of Tables

Table 2-1. Key features of hand dynamometers

Table 3-1. Finger length of adult surveyed by Size Korea. 302 males and females from 20 years and 69 years old are participated in this survey.

Table 3-2. Calibration Specification of force-torque sensor (Mini 45, ATI)

Table 3-3. Link length and its weight of driving part of the hand robot.

Table 3-4. Analysis result by ForceEffect™ according to MCP angle and applied force. (Unit: Nm)

Table 3-5. The variation of torque due to angle and magnitude error of applied force at MCP angle 0°. (Unit: Nm)

Table 3-6. The variation of torque due to angle and magnitude error of applied force at MCP angle 30°. (Unit: Nm)

Table 3-7. The variation of torque due to angle and magnitude error of applied force at MCP angle 60°. (Unit: Nm)

Table 4-1. Measure torque at F/T sensor when force is applied to the end-point of the hand robot at MCP angle 0°. (Unit: Nm)

Table 4-2. Measure torque at F/T sensor when force is applied to the end-point of the hand robot at MCP angle 30°. (Unit: Nm)

Table 4-3. Measure torque at F/T sensor when force is applied to the end-point of the hand robot at MCP angle 60°. (Unit: Nm)

Table 4-4. Average and standard deviation of all measured torque at all MCP angles. (Unit: Nm)

Table 4-5. Average of angle error due to applied force at MCP angle. Average and standard deviation are displayed in this table. (Unit: degree)

Table 4-6. Difference between analysis and experiment result according to applied force and MCP angle. (Unit: Nm)

Table 4-7. MCP angle deviation due to applied force. (Unit: degree)

Table 4-8. Modified analysis result according to applied force and MCP angle deviation. (Unit: Nm)

List of Figures

Figure 2-1 Hand's joints and their digits.

Figure 2-2. Goal of impedance control

Figure 3-1. The developed hand exoskeleton robot (a) top view and (b) side view

Figure 3-2. Hand robot control computer

Figure 3-3. Control box of the hand robot

Figure 3-4. Motor and force-torque sensor on top of the hand robot

Figure 3-5. Algorithm concept of the hand rehabilitation robot program

Figure 3-6. Program source code for ROM selection.

Figure 3-7. Source code for figuring out and printing maximum torque and force

Figure 3-8. Simple kinematics of the hand robot. Orange triangle represents ternary link and blue line for a link. Fixed joints are described as black.

Figure 3-9. One static example on ForceEffect™

Figure 3-10. One kinematics example on ForceEffect™

Figure 3-11. Kinematic drawing on ForceEffect™. Link length and weight are applied for each link. Red arrow represents reaction force at a fixed joint and yellow shows gravity force on each link. Reaction force due to gravity is indicated at each fixed joint (A, D, and F) and moment at joint A is also indicated. There is F/T sensor behind the gear (marked as black circle) and it is on the same axis line of the gear. Further information will be found in Figure 3-6

Figure 3-12. Gravity effect on the hand robot system according to MCP angle when 2kgf force is applied to the end-point of the hand robot. X axis represents MCP angle (degree), Y axis represents torque (Nm). As MCP angle increases, gravity effect on the hand robot becomes smaller. Also, At MCP angle 0°, gravity effect is the largest (0.107Nm) while it becomes smallest at MCP angle 60° (0.031Nm).

Figure 3-13. Schematic diagram of the hand robot at MCP angle (a) 0° (b) 30° (c) 60°. All forces are described in this Figure with blue, yellow, and red color. Blue = applying force, yellow = gravity force on each link, and red = reaction force or moment on fixed link. (Unit = N - force, Nm - moment)

Figure 4-1. Experiment with digital dynamometer under different MCP angles (a) 0° (b) 30° and (3) 60° Yellow solid line represents position vector r that connects MCP joint and fingertip. Dashed line shows reference line which indicates MCP angle.

Figure 4-2. One example of recorded data when force is applied to the hand robot. Dashed line represents the interval which data is acquired. Solid line is torque value measured by F/T sensor.

Figure 4-3. Comparison with analysis and experimental condition. Left picture shows before applying force to the hand robot which is analysis condition and right picture shows after applying 5kgf to the hand robot. Red line means reference and blue means the change of link structure after applying 5kgf.

Figure 4-4. Marker setup for tracing the trajectory while applying force to the end-point of the hand robot. 8 markers are attached to end-point, MCP joint, gear, and robot frame. The markers circled as red are interested in this experiment.

Figure 4-5. VICON camera setup for tracing the markers attached to the hand robot. 4 camera were used in this experiment. Camera position in 3D space is described for 4 cameras. In the middle of the screen, markers are positioned as a white sphere.

Figure 4-6. Modified link structure according to MCP angle deviation due to applied force. (a) MCP angle at 0° (b) MCP angle at 30° (c) MCP angle at 60°.

Figure 4-7. Linear fitting with modified analysis results and experiment results. X axis represents analysis result and y axis for experiment result. Among 5 data, maximum and minimum values are extracted so that three experiment results are matched to one analysis result.

Figure 5-1. Picture of wearing hand robot

I. INTRODUCTION

1.1 Purpose of Research

Many people suffer from diseases including neurological disorder, cardiac diseases, physical impairments, and others. Among them, there are some regions that need rehabilitation such as brain injury for survivors. Before providing therapy to them, assessment for them should be conducted for diagnosis and better rehabilitation. In case of hand rehabilitation, spasticity, passive range of motion (PROM), active range of motion (AROM), and grip force are the measurement target in order to evaluate their hand condition. For example, a dynamometer is used for measuring grip force and a goniometer is for range of motion. There is a strongly need for objective and quantitative diagnosis because it provides helpful insight about the effect of stroke on a hemiplegic limb and it may lead to a better rehabilitation therapy [1].

A novel hand rehabilitation robot hardware prototype is developed in authors' laboratory for the following purposes: the estimation of range of motion and force for both hand and wrist; the rehabilitation of hand and wrist. In terms of kinematics and mechanism, this hand robot applies six-bar mechanism for driving hand part and it is defined as a serial platform manipulator that two ternary links (platform) are connected by a single hinge. In the control aspect, time delay control (TDC) and impedance control are applied to the hand robot. For impedance control, validated force and theta are needed.

Either estimation or rehabilitation by the hand robot; however, force measured by force torque sensor (F/T sensor) is not verified so that it is essential to identify whether the force data is reliable or not. In order to assure that the grip force obtained by F/T sensor is considered as real human grip force, first of all, the comparison between the force data of F/T sensor and that of validated measurement tool for human grip force, dynamometer, has to be ensure. Therefore, the main issue of this thesis is the validation of the force measured by F/T sensor by identifying the relationship between the force data by F/T sensor and that by dynamometer. By ascertaining the relationship, the force of F/T sensor is reliable to estimate the condition of one's hand so that rehabilitation by the hand robot will be effectively conducted to the patients.

1.2 Structure of Thesis

This thesis consists of the following:

Chapter 2 provides a literature background that establishes the foundation of this research. Stroke is demonstrated and hand joint anatomy is described briefly for better understanding of terminology used throughout this thesis. A description of the neurological hand impairment following stroke is given shortly. In addition, this chapter introduces grip force measurement tools and methods. Contemporary grip force measurement concepts in the medical field are provided. Also, it illustrates diverse grip force measurement using various tools.

Chapter 3 demonstrates the measurement of grip force by dynamometer. It covers equipment explanation and validation of dynamometer's reliability. Plan for measuring human MCP joint torque using dynamometer will be explained and some issues are discussed with regard to measuring human MCP joint torque. Also, this chapter introduces the developed hand rehabilitation robot in the author's laboratory including its hardware and software. In addition to that, kinematics and mechanism of the hand rehabilitation robot will be illustrated. Finally, force analysis of the hand robot by using novel simulation tool, ForceEffect™ is described.

Chapter 4 explains experiments and their results. Verification of torque using hand robot is proceeded. Experimental setup and tasks are described shortly and after obtained data, data analysis are illustrated. Then, discussion of experiment results is covered. Analysis of experimental results with ForceEffect™ results is described, providing demonstration of the relationship between two results.

Chapter 5 concludes this research. Summary of this thesis is covered and some constraints during research are discussed. Finally, further works of this study are presented.

II. BACKGROUNDS

2.1 Stroke

A stroke, known as cerebrovascular accident (CVA), is the loss of brain function due to a disorder in blood supplement to the brain which leads to chronic physical disability or death. Strokes can be categorized by either ischemia (lacking of blood flow) or hemorrhage (bleeding). Ischemic strokes occur due to a lack of blood supply to part of the brain whereas hemorrhagic strokes are caused by a weakened vessel that ruptures or bleeds into the surrounding brain. Depending on the affected area, a range of impairments can appear: hemiparesis, partial paralysis, invisibility on one side of visual field, or dullness of apprehension or inability to articulate speech.

Generally, there are three main stages of strokes that can be classified by the time after onset. The time ranges representing these stages vary in literature, but mostly the first three to seven days are referred as the acute stage. The first one to six months are defined as the subacute stage, and the chronic stage starts after three or six months later in most cases [2].

According to mortality statistics of the World Health Organization in 2008 [3], stroke (10.8%, 615 million) was the third leading cause of death. Approximately 50% of stroke survivors undergo chronic hemiparesis and roughly 25% of them become dependent in activities of daily living (ADL) such as eating, dressing, or bathing [4]. Because of that, stroke patients usually have impairments on their upper extremity or lower extremity. Although affecting the neurological system, in most cases, the motor system is commonly affected by stroke [5]. 30-66% of chronic stroke patients with hemiparesis have poor arm function [6] and stroke victims usually have non-functional hand at least one hand, experiencing delays in grasping and opening their hands.

2.2 Hand Joint Anatomy

It is essential to review the hand anatomy in order to give better understanding of this thesis, especially focusing on the names of each joint. The digits of the hand are referenced by a number: the thumb (1st digit), the index finger (2nd digit), the middle finger (3rd digit), the ring finger (4th digit) and the small finger (5th digit). The thumb is composed of three joints from proximal to the wrist to the distal joint: the carpometacarpal joint (CMC), the metacarpal phalangeal joint (MCP) and the inter phalangeal joint (IP). The rest of the fingers have three joints called, the metacarpal phalangeal joint (MCP), the proximal inter phalangeal joint (PIP) and the distal inter phalangeal joint (DIP). The hand joint anatomy is illustrated in Figure 2-1 [7]. Through this study, these abbreviations will be frequently referred especially MCP.



Figure 2-1 Hand's joints and their digits [7].

2.3 Neurological Hand Impairment Following Stroke

In order to support the importance of hand rehabilitation, this thesis provides the mechanisms of hand impairment following stroke.

Generally, after experiencing stroke patients usually have hand motor impairment. For instance, muscle shrinking in the hand provokes hand weakness. Shortening of muscle tendons and contractures can reduce the range of motion (ROM) of the hand. Though such changes can adversely affect ROM of the hand, neurological mediated impairment such as spasticity and muscle weakness are the most responsible for hand function.

Following stroke, the flexor muscles of the hemi paretic hand become spastic, attenuating voluntary active extension. Spasticity is a condition that has a resistance to externally imposed movement with increasing speed of stretch and varying with the direction of joint movement [8]. Also, it rises rapidly above a threshold speed or joint angle and can increase muscle tone, or stiffness. One research has shown that the flexor spasticity was seen at the onset of movement of faster extension stretches but during flexion stretching few spasticity was measured [9].

2.4 Grip Force Measurement Tools

Grip force measuring has been used in clinical areas and for some purposes such as following:

1. To assess of upper limb impairment.
2. To evaluate work capacity for those with hand injuries and other work-related injuries.
3. To estimate the people with other impairments and disabilities, such as chronic fatigue syndrome, developmental disabilities and stroke.
4. To determine the efficacy of different treatments for people with a range of disabilities.

A variety of instruments is available to measure both static and dynamic grip force; however, most of them are to measure static grip force. Grip force measurement devices can be divided into 4 basic categories shown in Table 2-1 [10]-[14]. This table shows the main features of different types of dynamometer. Since hydraulic type of dynamometer used in this study, it is beyond the scope of this research to detail the mechanics and physics of how these instruments operate.

Table 2-1. Key features of hand dynamometers

Instrument type	Hydraulic	Pneumatic	Mechanical	Strain
Measures	Grip strength	Grip pressure	Grip strength	Grip strength
Based on	A sealed hydraulic system that enables grip strength to be read off a gauge dial	The compression of an air-filled compartment, e.g. A bag or bulb	The amount of tension produced in a spring	The variation in electrical resistance of a length of wire due to the strain applied to it
Example of instrument	Jamar	Martin Vigorimeter	Harpenden Dynamometer	Isometric Strength Testing Unit
Units	Kilograms (kg) or pounds of force (lb.)	Millimeters of mercury (mmhg) or pounds per square inch (psi) (lb./in ²)	Kilograms (kg) or pounds of force (lb.)	Newtons of force (N)
Advantages	Portable, economical, large amount of normative data available	Gentler on weak or painful joints	No evidence for superiority presented in the literature	Are not subject to leaks (of oil/water/air), which can compromise accuracy
Limitations	Can cause stress on weak joint. Can develop slow leaks and hysteresis	These instruments measure grip pressure, which is dependent on the surface area over which the force	Reproducibility of the grip force measurements is limited due to difficulties in exactly replicating the grip position and in calibrating the device	Can be expensive and heavy

Among those dynamometers, Jamar dynamometer is commonly used and selected as the standard by other dynamometers. A review of the reliability and validity of the Jamar system in comparison with other grip force measurement devices concluded that excellent inter-instrument reliability exists between the Jamar, Dexter and Baseline dynamometers and could be used interchangeably.

2.5 Impedance Control

In this thesis, impedance control is not mainly discussed but it is necessary to mention in shortly thus, basic concept of impedance control will be explained. Impedance control, an approach to the control of dynamic interaction between a manipulator and its environment, was proposed by Neville Hogan in 1985 [15]. And there were two objectives of impedance control such as following:

1. To achieve high-performance that responds to environmental contact force and
2. To control of dynamic behavior.

The goal of impedance control is to achieve desired impedance dynamics. Desired impedance dynamics can be expressed as follow:

$$M_d(\ddot{x}_d - \ddot{x}) + B_d(\dot{x}_d - \dot{x}) + K_d(x_d - x) = F_e$$

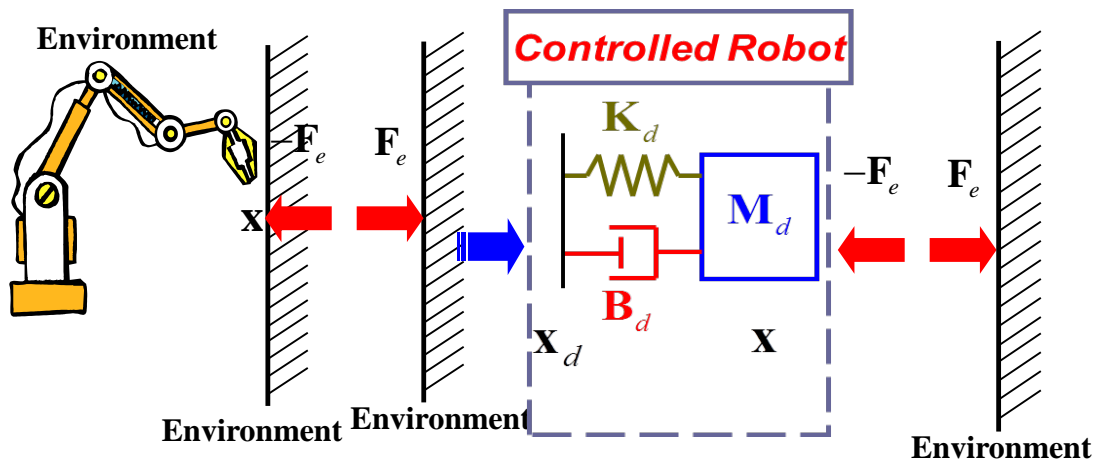


Figure 2-2. Goal of impedance control

where M_d , B_d , K_d is desired mass, damping, and stiffness parameters. \ddot{x}_d , \dot{x}_d , x_d is desired acceleration, velocity, and trajectory. \ddot{x} , \dot{x} , x is robot end-effector acceleration, velocity, and position. F_e is an interaction force on the environment exerted by the robot. As Figure 2-2 is shown, controlled robot behaves like the system that has mass, spring, and damping. The performance of the robot depends on how mass, stiffness, and damping parameters are designed: free motion or constrained motion. For example, if mass parameter is high, then a robot behaves very heavy thus robot seldom moves even though external force is

applied to the robot. On the other hand, if mass parameter is low, then a robot can be moved by external force easily. Free motion of the robot can be obtained by Therefore, by tuning those parameters either high, low or even zero, the performance of the robot is significantly different.

In order to achieve high performance with impedance control in a certain system, trajectory x and force F_e needs to be reliable. For the 1 degree of freedom (DOF) hand robot, trajectory can be replaced by angle θ and it can be sensed by encoder, which will be discussed in later chapter. Meanwhile, external force F_e also can be measured by Force-Torque sensor (F/T sensor) but the force information is not verified yet. Thus, as the purpose of this research, force sensed from F/T sensor needs to be confirmed as reliable data in order to realize impedance control into the hand rehabilitation robot.

In the following chapter, the measurement of hand grip force using dynamometer will be explained including equipment explanation and validation of its reliability. Also, the developed hand rehabilitation robot in author's laboratory will be introduced subsequently.

III. METHODS AND ANALYSIS

3.1 Introduction to the Developed Hand Rehabilitation Robot

In this chapter, hand rehabilitation robot developed in authors' laboratory will be introduced in detail. First, our developed hand robot will be explained in terms of hardware and software. Second, for better understanding of chapter 4, force analysis of the hand robot are conducted with free simulation tool named ForceEffect™.

3.1.1 Hardware

A novel hand rehabilitation robot hardware prototype is developed in authors' laboratory for both the rehabilitation of patients with neurological disorder such as stroke as shown Figure 3-1 as below.

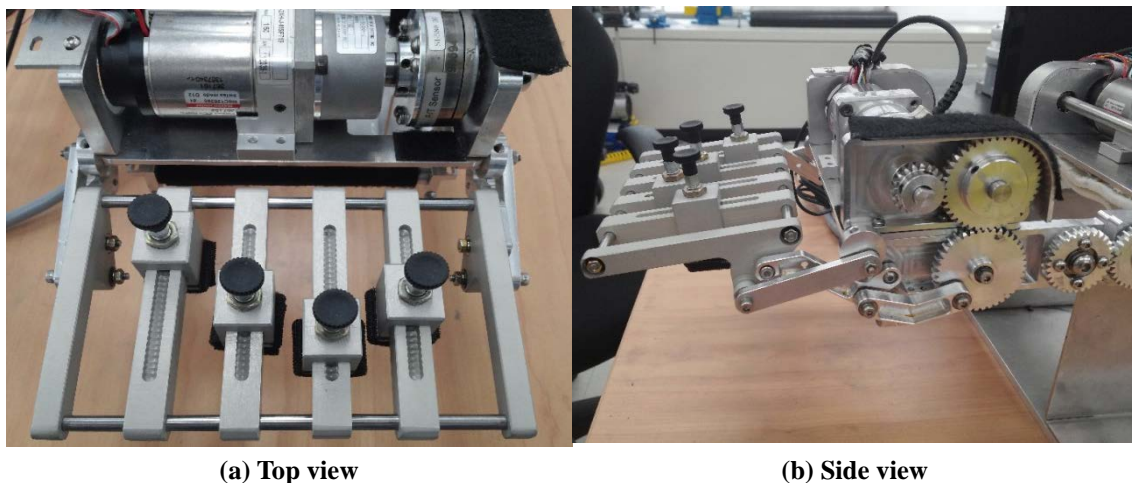


Figure 3-1. The developed hand exoskeleton robot (a) top view and (b) side view

There are notable features of the hand robot in terms of mechanism, structures, and training mode. First of all, this hand robot is capable of adjusting finger holding part by using a plunger as shown in Figure 3-1. A plunger can freely move along the 70mm-bar with holes at intervals of 1mm which can accommodate various finger length. To figure out how much range it can cover, finger length of people was investigated. According to the 6th Korean anthropometric survey report in 2010 [17], except for thumb, finger length of 302 people whose age is from 20 years to 69 years old is measured and its result is listed on Table 3-1 as below. As it is described, the maximum finger length is about 91mm and the minimum finger length is less than 44mm. Since the distance between robot frame and plunger is more than 50mm and less than 120mm approximately and the difference

between maximum and minimum of each finger length is less than 30mm, thus most of subject can be fitted on our hand robot by just adjusting plunger. Once fingertip position is determined according to finger length, then place the plunger for appropriate position of each finger. After adjusting plunger, each finger is fixed by Velcro strap.

Table 3-1. Finger length of adult surveyed by Size Korea. 302 males and females from 20 years and 69 years old are participated in this survey.

	Index	Middle	Ring	Little
AVG ± SD (mm)	68.7±4.72	76.42±5.02	71.86±6.57	56.95±5.89
Maximum (mm)	81.08	91.41	85.03	70.55
Minimum (mm)	55.49	63.82	58.44	43.96

Second, in terms of mechanism, whole finger parts are driven by one DC motor. By utilizing gears and crossed 4-bar link mechanism, it enables the hand robot to be operated with 1 DOF, providing full hand grasping motion. Currently, only four finger parts are operated and later thumb part will be designed without adding any other motor.

Third, passive and active training modes are available for hand rehabilitation. In passive mode, hand robot follows the desired trajectory. Robot trajectory can be modified by subject. If subject didn't have enough ROM, subject could feel pain due to the training with excessive ROM. Thus, it is reasonable to have options for choosing ROM in order to offer the suitable training to each subject. In addition, users can also select the robot speed such as 1Hz, 0.5Hz, and 0.25Hz before initiating training. It is usually determined by subject's hand condition such as contracture or spasticity. In active mode, the robot impedance can be adjusted to one of three options: low, medium, and high impedance. As robot impedance gain is selected, the robot operates either assistive or resistive motion.

Figure 3-2 displays electronics panel that contains the hardware needed to output command signals to a motor and receive input signals from a motor, a torque sensor and an encoder. Power supply units (Switching DC Power Supply, SPS 606, Good Will Instrument Co., Ltd) provides power to the motor and torque sensor and has output voltage range from 0 to 60V. The motor is controlled by a motor driver (Maxon Motor Control, 4-Q-EC Amplifier, DEC 70/10). Two different data acquisition (DAQ) board are installed to convert both torque sensor input signal and motor input signal to digital signals. In addition, control box for the hand robot is customized for convenience of transportability as shown in Figure 3-3.



Figure 3-2. Hand robot control computer



Figure 3-3. Control box of the hand robot

A DC, brushless motor (EC-i 40, Maxon motor) in series with harmonic drive (CSF-11-50, Sam-ik THK, gear ratio 50:1) was chosen for driving four finger parts. For selecting desired motor, it is referred the 1DOF cable-driven hand robot [18] in authors' laboratory, indicating that nominal torque was 3.44Nm. If the input current of the motor amplifier becomes high, motor output torque can be more than 3.44Nm. Further explanation of how to choose the required torque for the hand robot is written in the paper [18].

An Encoder MR by Maxon motor (500 counts), mounted on the motor, was used for position, velocity, and acceleration sensing of MCP joint angle. It has three channels and the resolution of this encoder is 0.72°/count.

A 6-axis force-torque sensor (Mini 45, ATI) is positioned between the motor and the linkages as shown in Figure 3-4. This F/T sensor has a wide range of measurement in force and torque as shown in Table 3-2. At F/T sensor, torque generated by human hand can be measured and real-time force and torque is updated in the hand robot control computer.

According to previous study of measuring grip force for stroke patients [19], affected hand grip force of 15 stroke patients whose hand ratio range is 11 to 82% was measured by dynamometer and its average is around 135N. Considering the maximum grip force (216N) and the minimum grip force (34N), our hand robot can sufficiently cover those ranges. However, the posture that they measured grip force is different from the way we use. Only difference in posture is wrist position, so it doesn't affect maximum grip force significantly.

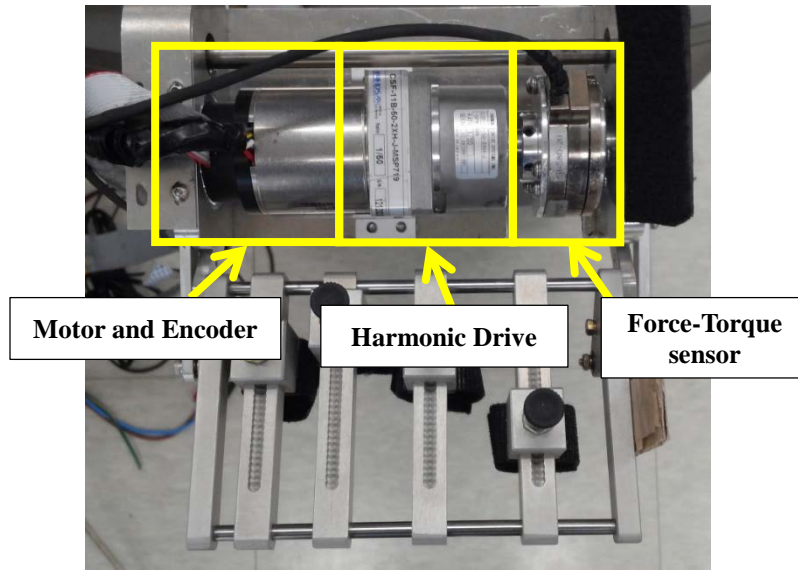


Figure 3-4. Motor and force-torque sensor on top of the hand robot

Table 3-2. Calibration Specification of force-torque sensor (Mini 45, ATI)

Calibration	F _x , F _y	F _z	T _x , T _y	T _z	F _x , F _y	F _z	T _x , T _y	T _z
SI-580-20	580N	1160N	20Nm	20Nm	1/4N	1/4N	1/188Nm	1/376Nm
	Sensing Ranges				Resolution			

3.1.2 Software

The hand rehabilitation robot is controlled with customized software program developed by author's laboratory. For the real-time control of the hand robot, Linux fedora 11 is installed and then, the RealTime Application Interface for Linux (RTAI) 3.8 and COMEDI drive 0.8.1 are mounted. Under the real-time environment, customized program is developed for the newly developed hand rehabilitation robot. In this session, its algorithm will be introduced including control and other optional functions.

Overall algorithm is adopted from the previous version of the hand robot [17] in author's laboratory and modified. Unlike to previous version, mode selection, gain selection for impedance control, and ROM selection are newly added. Gain selection for impedance control will be covered later because it is not verified yet. The concept of algorithm is simply described in Figure 3-5 as below.

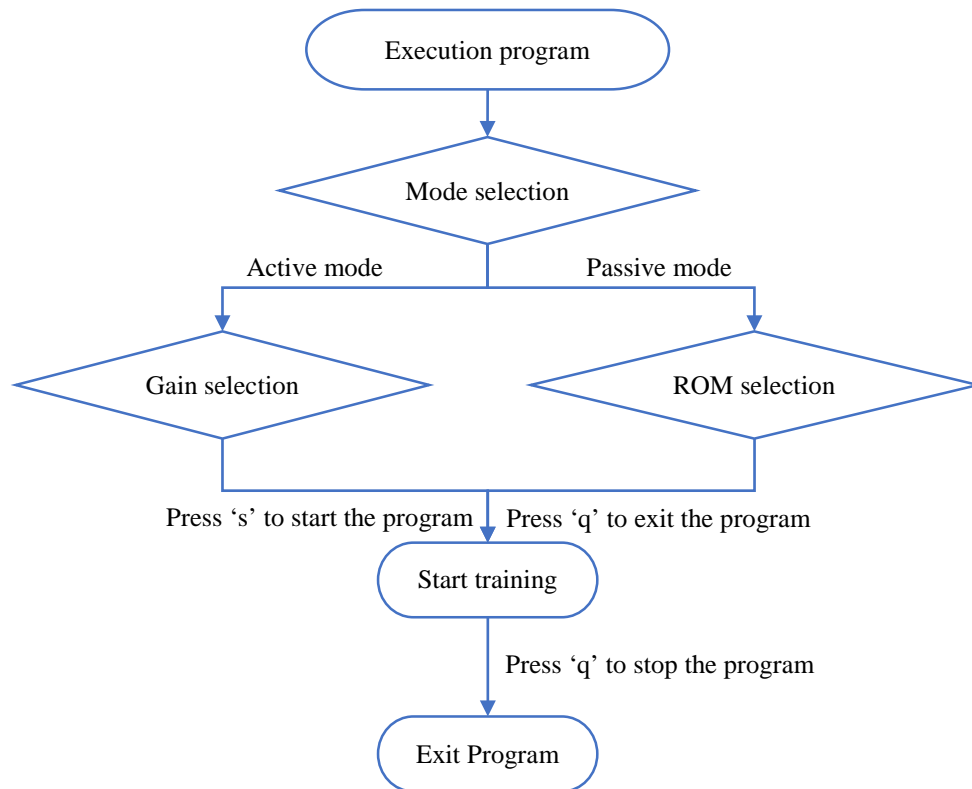


Figure 3-5. Algorithm concept of the hand rehabilitation robot program

After running the program in command window, user can select mode either active or passive according to the purpose of the hand therapy. Then depending on the subject's hand condition, ROM is selected from 10° to 90°. Mostly, stroke patient doesn't have large ROM because of contracture and spasticity, thus various ROM needs to be provided. Figure 3-6 shows the program source code for ROM selection. In this source, five different ROM can be available and of course it can be changeable along with patient's condition.

In order to display the maximum grip force of the subject on the command window, Algorithm part for finding maximum torque and printing it during active mode is programmed as follow:

1. variable declaration (temp_FT[0], max_FT[0])
2. every sampling time (1ms) collect torque values (torque information is in FT_data[5])
3. it stores in temporary array (temp_FT[0])
4. compare temporary array with maximum torque array
5. if temp is bigger than max, put temp data into max

```

if(mode=='1'){
// passive mode
printf("\n\nselect ROM!");
printf("\n1) 10  2) 20  3) 30  4) 60  5) 90:");
while(1){
ROM_mode = getch();
if(ROM_mode == '1'){
//_____ROM choose-!
thf = -10.0+(cv+2.0); // hand theta final [rad] :: (-) for extension (+) for flexion
thf2 = 0.0+(cv+2.0); // wrist theta final [rad]
break;
}
else if(ROM_mode == '2'){
//_____ROM choose-!
thf = -20.0+(cv+2.0); // hand theta final [rad] :: (-) for extension (+) for flexion
thf2 = 0.0+(cv+2.0); // wrist theta final [rad]
break;
}
else if(ROM_mode == '3'){
//_____ROM choose-!
thf = -30.0+(cv+2.0); // hand theta final [rad] :: (-) for extension (+) for flexion
thf2 = 0.0+(cv+2.0); // wrist theta final [rad]
break;
}
else if(ROM_mode == '4'){
//_____ROM choose-!
thf = -60.0+(cv+2.0); // hand theta final [rad] :: (-) for extension (+) for flexion
thf2 = 0.0+(cv+2.0); // wrist theta final [rad]
break;
}
else if(ROM_mode == '5'){
//_____ROM choose-!
thf = -90.0+(cv+2.0); // hand theta final [rad] :: (-) for extension (+) for flexion
thf2 = 0.0+(cv+2.0); // wrist theta final [rad]
break;
}
else printf("\n\nwrong input! please select one of those!\n 1) 10  2) 20  3) 30  4) 60  5) 90:");
}; // ROM selection while loop end for

```

Figure 3-6. Program source code for ROM selection.

And Figure 3-7 describes the source code for figuring out the maximum torque during grasping the hand robot and also printing it on the command window. Since F/T sensor senses force and torque at all three axis, force at x, y, and z axis are measured as well as torque. The maximum torque is printed on the command window just as the program is shut down.

```

for(i=0; i<cnt; i++){
// modified by jihyuk Park 2013. 4. 2          POWER MEASUREMENT SOURCE CODE
temp_FT = record_data[1][i];
temp_FT2 = record_data[2][i];
temp_FT3 = record_data[3][i];
temp_FT4 = record_data[4][i];
temp_FT5 = record_data[5][i];
temp_FT6 = record_data[6][i];

if (temp_FT < 0)    temp_FT = -temp_FT;
if (temp_FT2 < 0) temp_FT2 = -temp_FT2;
if (temp_FT3 < 0) temp_FT3 = -temp_FT3;
if (temp_FT4 < 0) temp_FT4 = -temp_FT4;
if (temp_FT5 < 0) temp_FT5 = -temp_FT5;
if (temp_FT6 < 0) temp_FT6 = -temp_FT6;

if (temp_FT > max_FT)
max_FT = temp_FT;
if (temp_FT2 > max_FT2)
max_FT2 = temp_FT2;
if (temp_FT3 > max_FT3)
max_FT3 = temp_FT3;
if (temp_FT4 > max_FT4)
max_FT4 = temp_FT4;
if (temp_FT5 > max_FT5)
max_FT5 = temp_FT5;
if (temp_FT6 > max_FT6)
max_FT6 = temp_FT6;

// POWER MEASURE 결과값 출력하기!
if(mode == '2'){
printf("\nPOWER MEASUREMENT RESULT");
printf("\nMaximum force:  %f  %f  %f  %f  %f  %f  \n\n",max_FT, max_FT2, max_FT3, max_FT4, max_FT5, max_FT6);
}

```

Figure 3-7. Source code for figuring out and printing maximum torque and force

3.1.3 Kinematics and Mechanism of the Developed Hand Robot

Figure 3-8 shows simple kinematics of the hand robot. In the aspect of kinematic design, our hand robot has six-bar mechanism including two ternary link and is a serial platform manipulator type robot whose definition is that multiple platforms, which are two ternary links, will be connected by a single hinge. Two ternary links, expressed as orange, three links, expressed as blue line, and a hidden link that connects the entire base, expressed as black, altogether is six bars.

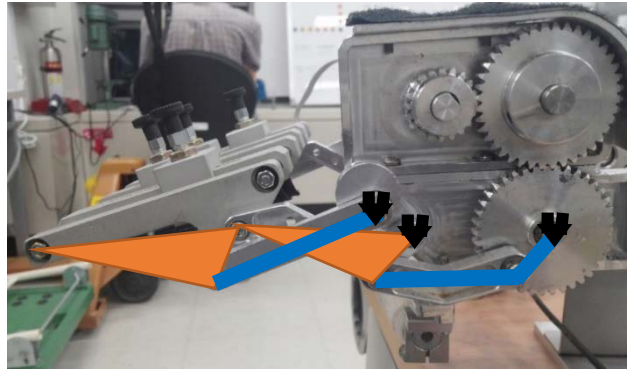


Figure 3-8. Simple kinematics of the hand robot. Orange triangle represents ternary link and blue line for a link. Fixed joints are described as black.

3.1.3.1 Verification of Its Mobility by Grübler's and Alizade's Formula

In order to verify the DOF of our hand robot, the Grübler's and Alizade's mobility formulas are used. Grübler's mobility formula is the most commonly used equation for evaluating simple linkages. Grübler's mobility formula is given as

$$M = 3(N - 1) - 2P_1 \quad (1)$$

where M is mobility, n is total number of links, and P_1 is total number of 1 DOF joints. In case of our hand robot, $n=6$, and $P_1=7$ so the eq. (1) will be $1 = 3(6 - 1) - 2 \cdot 7$

Alizade's mobility formula is given as

$$M = \sum f_i - 3L \quad (2)$$

Where M is mobility, f_i is total number of DOF of all joints and L is number of independent loop. Since $f_i=7$ and $L=2$ so that eq. (2) will be $1 = 7 - 3 \cdot 2$

Again, Alizade's mobility formula also shows that our hand robot has 1 DOF as the same as the result of Grübler's mobility formula. Therefore, the number of DOF of our hand robot is verified by those two mobility formula.

3.2 Analysis of the Developed Hand Rehabilitation Robot

Since analysis of the hand robot has not been done yet and in order to ensure the values read by F/T sensor as reliable information, its validation should be carried out. Suppose that the situation of measuring grasping force is considered as static situation. When exerted force is applied to the end-point of the hand robot, the hand robot is controlled by the system so that the displacement due to the exerted force is negligible.

For the analysis of the hand robot, simulation tool, Autodesk ForceEffect™ is used. Autodesk ForceEffect™ is a simple, intuitive analysis tool, offered as a free software so that anyone can download and simply install it either on the Google Chrome or the Internet Explorer. Also, it offers a report which contains equations and graphs that describes the analysis result. In this chapter, ForceEffect™ will be introduced shortly and then, force analysis of hand robot using ForceEffect™ will be followed.

3.2.1 Introduction to Analysis Tool, Autodesk ForceEffect™

ForceEffect™ offered by Autodesk is open software that can run on the Internet Explorer or the Google Chrome with simple installation. ForceEffect™ is suitable for static system analysis using free body diagrams and simple kinematics analysis is available also. Figure 3-9 shows an example of ForceEffect™. As shown in Figure 3-9, static analysis of bridge can be done easily by drawing of links on the sketch and making them connect with joints. Besides, kinematics also can be implemented as shown in Figure 3-10.

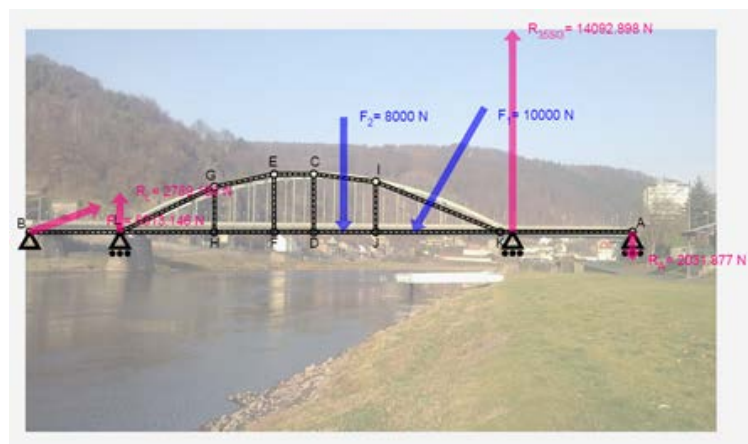


Figure 3-9. One static example on ForceEffect™

Especially, analysis result can be found through report in detail. The report describes all input values and output results for all elements. If an element is selected, the report includes only inputs and results related to the selected element. For equilibrium diagrams, the report lists equilibrium equations for every single element. The equations comprise moment balance ($\sum M = 0$) and force balance ($\sum F[X] = 0$ and $\sum F[Y] = 0$). First

three equations correspond to the element equilibrium. Other equations correspond to equilibrium of joints and supports attached to the element. In addition, shear force and moment diagram graph is located below equations.



Figure 3-10. One kinematics example on ForceEffect™

3.2.2 Force Analysis of the Hand Rehabilitation Robot using ForceEffect™

For static force analysis in ForceEffect™, several primary elements are considered: link length, link weight, MCP angle, direction and magnitude of the force. All these elements affect analysis output, i.e. torque, even considerably small change. Thus, in order to implement accurate and meaningful analysis, efforts to reduce the difference between analysis condition and experimental condition is definitely required.

First, the length and the weight of each link is measured. Each link length is measured by digital Vernier calipers and digital scale measures each link weight. Their results are listed on table 3-3. Despite of light weight of each link, link weight is considered because of gravity effect on links. Then, using side view capture image of the hand robot, link structure is drawn as shown in Figure 3-11 in order to make sure the joint position including fixed joints (A, D, and F in Figure 3-11) while MCP angle is changed as 0°, 30°, and 60° where MCP angle is defined as the angle between the segment that connects joint H and joint D in Figure 3-11 and x-axis, which is the horizontal line on Figure 3-11.

Table 3-3. Link length and its weight of driving part of the hand robot.

Link	H-E	H-G	G-E	G-F	E-C	E-D	C-D	C-B	A-B
Length (mm)	68.3	61.2	14.8	51.2	43.4	52.5	14.5	39.6	13.7
Weight (g)	12.3	11.1	2.7	6.5	2.6	3.2	0.9	6.6	*

* This link cannot be measured because link A-B composes of gear and link joint

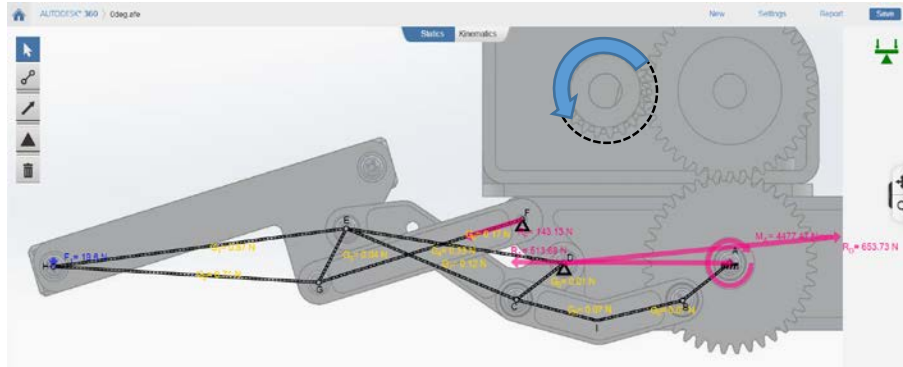


Figure 3-11. Analysis result of hand robot on ForceEffect™. Each link length and weight are applied. Reaction force (red) is depicted and gravity force (yellow) as well. Force is applied at joint H and resultant moment is indicated at joint A. Final output torque which can be measured by F/T sensor is represented as blue arrow. Further information will be found in Figure 3-4

Since gravity due to not only MCP angle but also link weight affects output torque, thus it cannot be ignored. In other words, as MCP angle increase, moment arm (segment HD in Figure 3-11) becomes shorter so that resultant moment at joint A naturally becomes smaller, indicating that moment at joint A has inverse relation with the magnitude of MCP angle. The moment due to gravity is shown in Figure 3-12. Gravity case is that link weight is considered and no gravity means that link weight is not considered. At MCP angle 0°, the difference between gravity and no gravity is maximum, 0.107Nm, and minimum, 0.041Nm, compared to other MCP angles. Of course, if applied force becomes larger such as 3kgf or 4kgf, gap between gravity and no gravity definitely gets larger. In conclusion, gravity affects moment in terms of MCP angle ranging from 0.107Nm to 0.041Nm under the same applied force and it.

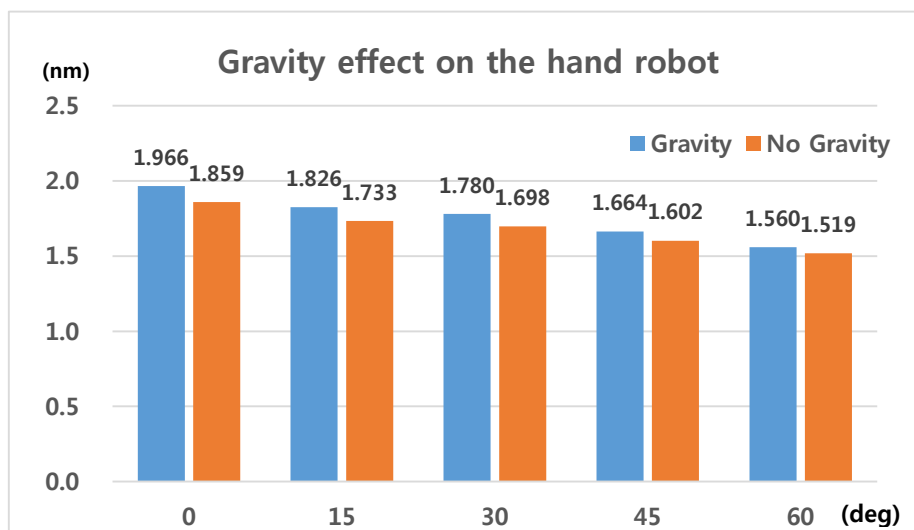
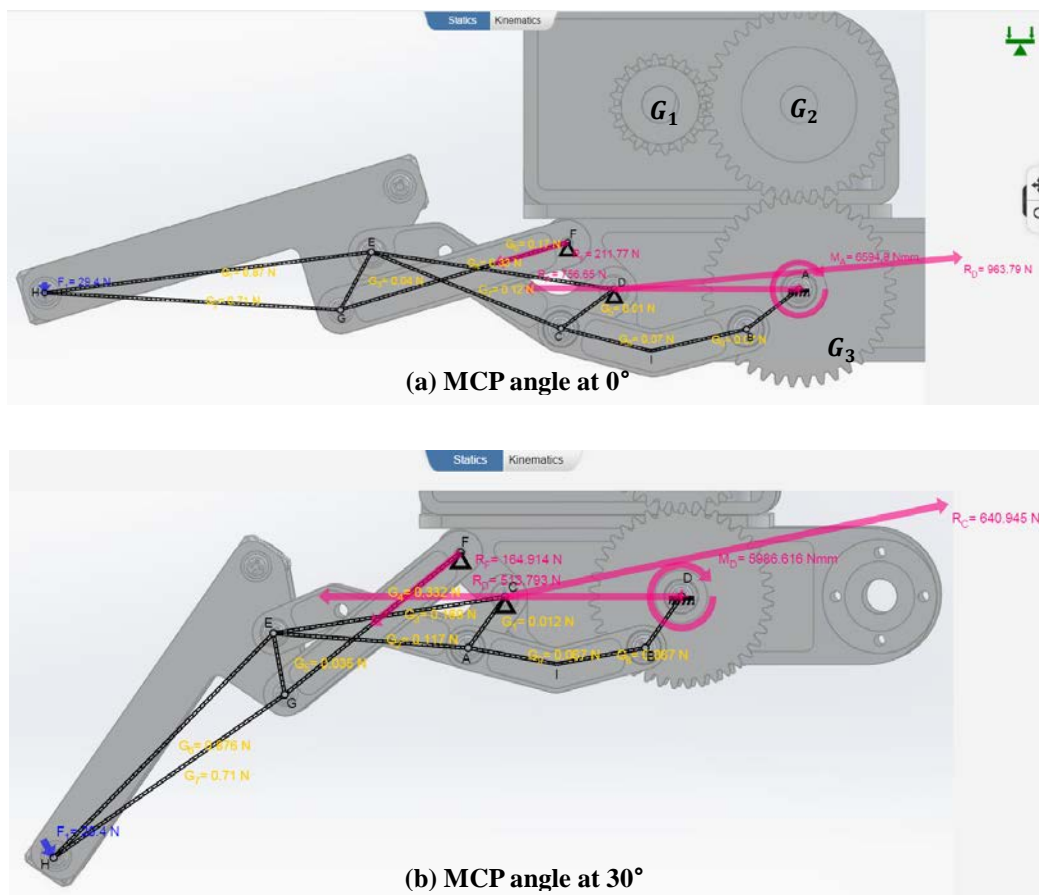


Figure 3-12. Gravity effect on the hand robot system according to MCP angle when 2kgf force is applied to the end-point of the hand robot. X axis represents MCP angle (degree), Y axis represents torque (Nm). As MCP angle increases, gravity effect on the hand robot becomes smaller. Also, At MCP angle 0°, gravity effect is the largest (0.107Nm) while it becomes smallest at MCP angle 60° (0.031Nm).

Second, MCP angle is also considered for the static force analysis of the hand robot. MCP angle is one of the key for the estimation of human MCP torque. As MCP angle changes, link structure is also changed as shown in Figure 3-13 so that it results the variation of reaction force at each fixed joint and resultant moment. Once the relation between torque sensed at F/T sensor and applied force to the endpoint of the hand robot is verified, human MCP torque and fingertip force can be inversely calculated by the relation. Therefore, it is significant to analyze how torque can be different due to the variation of MCP angle and to know the relation between torque and MCP angle.

Third, applied force to the endpoint of the hand robot is another major factor for static force analysis. In order to validate the relation between applied force and torque, three different forces such as 3kgf, 4kgf, and 5kgf are applied. The analysis results are shown in Table 3-4.



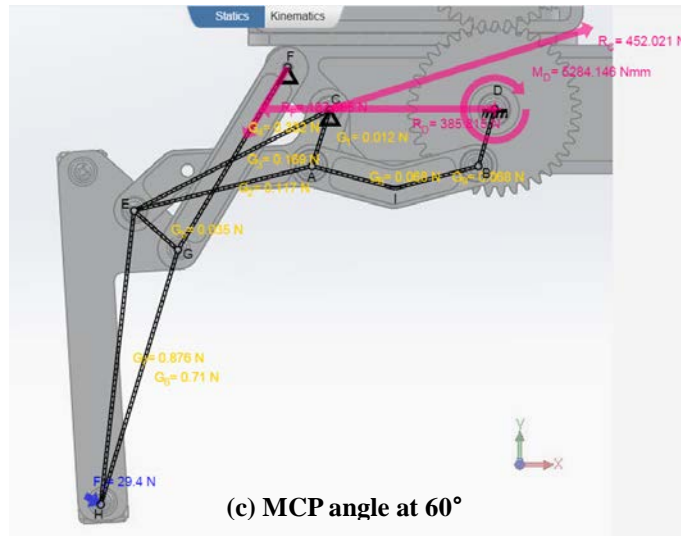


Figure 3-13. Schematic diagram of the hand robot at MCP angle (a) 0° (b) 30° (c) 60°. Blue arrow shows applying force, yellow for gravity force on each link, and red describes reaction force or resultant moment on fixed link. (Unit = N - force, Nm - moment)

Schematic diagram of the hand robot is described in Figure 3-13 according to MCP angle. Each link has its weight is applied as it is listed (See Table 3-3) thus, gravity is described on each link (yellow). Applied force on the end-point of the hand robot is represented (blue arrow) and its unit is N. As a result of applied force, reaction force and resultant moment at each fixed joint are also presented (red).

Table 3-4. Analysis result by ForceEffect™ according to MCP angle and applied force. (Unit: Nm)

MCP Angle	Applied Force	Resultant Moment
0°	3kgf	2.896
	4kgf	3.826
	5kgf	4.775
30°	3kgf	2.628
	4kgf	3.477
	5kgf	4.326
60°	3kgf	2.320
	4kgf	3.079
	5kgf	3.839

This resultant moment is calculated by multiplying gear ratio, 2.278, with moment at joint D (See Figure 3-13 (a)). Gear ratio can be calculated as follow:

$$\text{Gear ratio} = \frac{G_2}{G_1} \times \frac{G_3}{G_2} = 2.278$$

where G_1 , G_2 , and G_3 are the number of each gear tooth (See Figure 3-13 (a)).

Thus, after obtaining moment at G_3 from analysis, torque can be finally calculated by multiplying

gear ratio.

As it is demonstrated on table 3-4, at MCP angle 0° moment is larger than any other MCP angles under same applied force. It becomes smaller as MCP angle increases because moment arm is the longest at MCP angle 0° and becomes shorter as MCP angle increases.

3.2.2.1 The Effect of Magnitude and Angle error of Applied Force

In this session, the effect of magnitude and angle deviation of applied force will be covered. The purpose of this analysis is to identify error due to magnitude and angle deviation of applied force. It could possibly happen either by experimenter's mistake or reading error. Thus, it is required to investigate how much such errors could affect experimental output, torque.

In order to examine the effect, the two conditions are considered to analysis: the applied force has an error of 0.1kgf less or more than target force. Simultaneously, ±5° angle error of applied force is considered to analysis. Suppose that experimenter applies force less or more than target force to the end-point of the hand robot and at the same time, angle error occurs during applying force to the hand robot within 5°. From Table 3-5 to Table 3-7, the variation of torque due to angle and magnitude error of applied force is illustrated.

As it is expected, maximum torque surely occurs as applied force increases. Meanwhile, when angle of applied force is less than target angle, torque increases. It indicates that torque increases when the direction of force is interior to the hand robot and it decreases when the direction of force is exterior to the hand robot. Overall, the variation of torque has range between 0.096Nm to 0.142Nm. In conclusion, error of magnitude and angle of applied force could be a standard that determines whether experiment results are reliable or not.

Table 3-5. The variation of torque due to angle and magnitude error of applied force at MCP angle 0°. (Unit: Nm)

Angle error Applied force	-5°	0°	+5°
2.9kgf	2.806 (+0.003)	2.803	2.780 (-0.023)
3.0kgf	2.899 (+0.003)	2.896	2.872 (-0.024)
3.1kgf	2.992 (+0.003)	2.989	2.964 (-0.025)
3.9kgf	3.736 (+0.003)	3.733	3.701 (-0.032)
4.0kgf	3.829 (+0.003)	3.826	3.793 (-0.033)
4.1kgf	3.922 (+0.003)	3.919	3.886 (-0.033)
4.9kgf	4.666 (+0.005)	4.661	4.622 (-0.039)
5.0kgf	4.759 (+0.005)	4.754	4.714 (-0.040)
5.1kgf	4.852 (+0.005)	4.847	4.806 (-0.041)

Table 3-6. The variation of torque due to angle and magnitude error of applied force at MCP angle 30°. (Unit: Nm)

Angle error Applied force	-5°	0°	+5°
2.9kgf	2.558 (+0.014)	2.544	2.510 (-0.034)
3.0kgf	2.644 (+0.016)	2.628	2.594 (-0.034)
3.1kgf	2.729 (+0.016)	2.713	2.678 (-0.035)
3.9kgf	3.412 (+0.020)	3.392	3.348 (-0.044)
4.0kgf	3.498 (+0.021)	3.477	3.431 (-0.046)
4.1kgf	3.583 (+0.021)	3.562	3.515 (-0.047)
4.9kgf	4.266 (+0.025)	4.241	4.184 (-0.057)
5.0kgf	4.351 (+0.025)	4.326	4.268 (-0.058)
5.1kgf	4.436 (+0.025)	4.411	4.352 (-0.059)

Table 3-7. The variation of torque due to angle and magnitude error of applied force at MCP angle 60°. (Unit: Nm)

Angle error Applied force	-5°	0°	+5°
2.9kgf	2.266 (+0.022)	2.244	2.205 (-0.039)
3.0kgf	2.343 (+0.023)	2.320	2.279 (-0.041)
3.1kgf	2.420 (+0.024)	2.396	2.354 (-0.042)
3.9kgf	3.034 (+0.031)	3.003	2.951 (-0.052)
4.0kgf	3.110 (+0.031)	3.079	3.025 (-0.054)
4.1kgf	3.187 (+0.032)	3.155	3.100 (-0.055)
4.9kgf	3.801 (+0.038)	3.763	3.696 (-0.067)
5.0kgf	3.877 (+0.038)	3.839	3.771 (-0.068)
5.1kgf	3.954 (+0.039)	3.915	3.845 (-0.070)

IV. EXPERIMENTS AND RESULTS

4.1 Verification of Torque Using Hand Robot with Applied Force by Digital

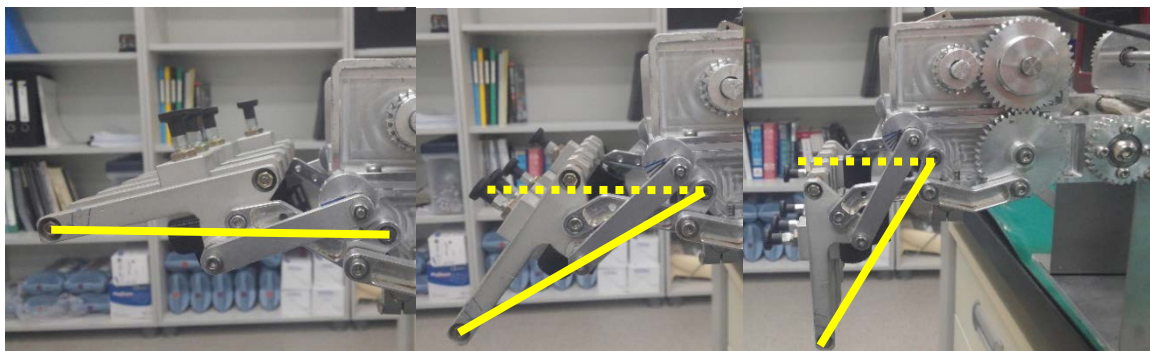
Dynamometer

In this chapter, for the verification of torque using hand robot, experiment with applied force using digital dynamometer is carried out. The purposes of this experiment are following:

1. To figure out the relationship between applied force and torque sensed by F/T sensor and
2. To check whether the analysis result is validated or not.

First, experimental setup and tasks are introduced. Data analysis before performing experiment is explained shortly. Then experiment results will be covered and discussion of experiment results will be provided.

4.1.1 Experimental Setup and Tasks



(a) MCP angle at 0°

(b) MCP angle at 30°

(c) MCP angle at 60°

Figure 4-1. Experiment with digital dynamometer under different MCP angles (a) 0° (b) 30° and (3) 60°

Yellow solid line represents position vector r that connects MCP joint and fingertip. Dashed line

To verify measured torque using hand robot, it is required to validate whether the torque value is reliable to use or not. In order to prove it, experiment is carried out at three different MCP angle such as 0° , 30° , and 60° as shown in Figure 4-1. The procedure of experiment is demonstrated as follow:

1. Set MCP angle as 0° and start the program to control the hand robot after experiment is ready
2. Using digital dynamometer, 3kgf force is applied to the end-point of the hand robot for about 3 seconds and measure the torque from F/T sensor
3. Repeat the whole procedure 5 times

Whole experiment procedure is repeated with 4kgf and 5kgf. For the safety, four 2.5kg barbells are placed on the hand robot plate not to move during experiment. In this experiment, time delay control (TDC) was used for position control. Control law of TDC is shown in equation (2) as follow.

$$\tau = \tau_{(t-L)} + \bar{M}(\ddot{e} + K_d\dot{e} + K_p e) \quad (2)$$

where τ is control input, which is torque, $\ddot{e} = \ddot{\theta}_d - \ddot{\theta}$, $\dot{e} = \dot{\theta}_d - \dot{\theta}$, $e = \theta_d - \theta$, \bar{M} , K_d , and K_p are constant gain respectively. L is sampling time. Thus, when force is applied to the end-point of the hand robot, links are rarely moved by applied force so that experiment condition is considered as static situation.

4.1.2 Data Analysis

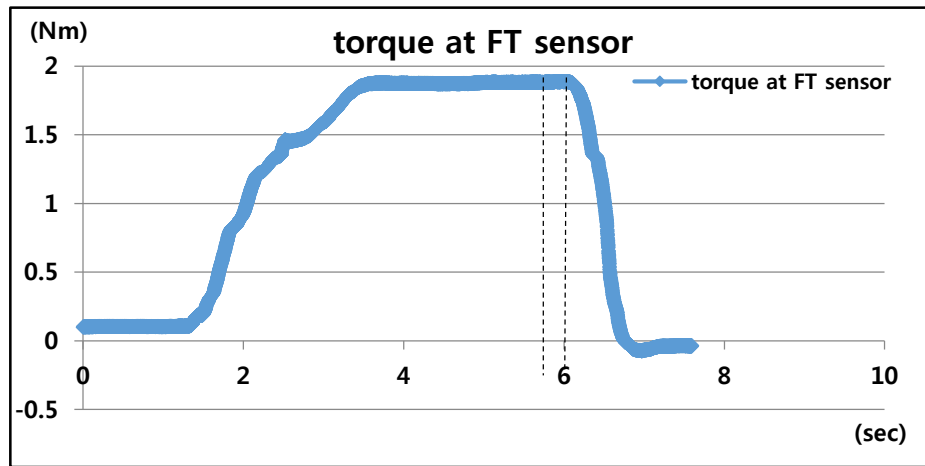


Figure 4-2. One example of recorded data when force is applied to the hand robot. Dashed line represents the interval which data is acquired. Solid line is torque value measured by F/T sensor.

Data analysis was performed using F/T sensor and encoder attached to motor. Customized program in hand robot's control computer recorded the torque measured by F/T sensor and angle data by encoder at sampling rate of 1 kHz. Data was recorded by code in customized program with sampling time of 1ms after initiating the program.

Figure 4-2 is one example of experimental result. Mostly, for the first 1-2 seconds force was not applied to the hand robot and for next 3 seconds force was applied. When it reached target force, maintained the force for about 2-3 seconds. After pressing 'q' for stop data was automatically saved as m-file which can be used in MATLAB® program. Dashed line represents the interval which data is acquired and solid line is torque value measured by F/T sensor. Among five different experiment results, maximum and minimum results are excluded, thus only three experiment results are reflected for the analysis. In conclusion, total 27 experiment results are used for analysis.

4.1.3 Experiment Results

Experiment results are listed in Table 4-1, 4-2, and 4-3. Each table is the result for MCP angle 0°, 30°, and 60° respectively.

Table 4-1. Measure torque at F/T sensor when force is applied to the end-point of the hand robot at MCP angle 0°. (Unit: Nm)

Applied force \ Trials	1st trial	2nd trial	3rd trial	4th trial	5th trial
3kgf	1.984	2.073	2.057	2.050	2.116
4kgf	2.635	2.659	2.881	2.664	2.691
5kgf	3.427	3.345	3.373	3.475	3.326

Table 4-2. Measure torque at F/T sensor when force is applied to the end-point of the hand robot at MCP angle 30°. (Unit: Nm)

Applied force \ Trials	1st trial	2nd trial	3rd trial	4th trial	5th trial
3kgf	2.305	2.118	2.037	2.183	2.075
4kgf	2.829	2.847	2.927	2.829	2.855
5kgf	3.283	3.376	3.450	3.394	3.306

Table 4-3. Measure torque at F/T sensor when force is applied to the end-point of the hand robot at MCP angle 60°. (Unit: Nm)

Applied force \ Trials	1st trial	2nd trial	3rd trial	4th trial	5th trial
3kgf	1.963	1.980	1.995	1.966	1.896
4kgf	2.587	2.506	2.595	2.654	2.693
5kgf	3.230	3.108	3.148	3.285	3.073

Table 4-4. Average and standard deviation of all measured torque at all MCP angles. (Unit: Nm)

Applied force \ MCP angle	0°	30°	60°
3kgf	2.060±0.009	2.125±0.044	1.970±0.007
4kgf	2.671±0.014	2.844±0.011	2.612±0.030
5kgf	3.382±0.034	3.359±0.038	3.162±0.051

Average and standard deviation of all measured torque except maximum and minimum result for each case is displayed in Table 4-4 as above. As it is demonstrated, measure torque is the highest at MCP angle 30°, and the lowest at MCP angle 60°. Compared to analysis results which show that magnitude of torque becomes smaller as MCP angle increases, experiment results have apparently contradictory result for the case of maximum torque while have the same result as analysis result for the case of minimum torque.

And average of angle error due to applied force is listed on Table 4-5. Angle error is defined as the difference between current theta and desired theta and it is measured when force is applied at each MCP angle.

As it is demonstrated, angle error is below 0.03° which means that it can be ignored.

Table 4-5. Average of angle error due to applied force at MCP angle. Average and standard deviation are displayed in this table. (Unit: degree)

MCP angle Applied force	0°	30°	60°
3kgf	0.003±0.018	0.012±0.031	0.008±0.023
4kgf	0.029±0.013	0.020±0.021	0.008±0.025
5kgf	0.003±0.021	0.020±0.017	0.025±0.013

The difference between analysis result and experiment result is listed on Table 4-6. Comparing other cases at MCP angle 30° and 60° , the difference between analysis and experiment result is the highest. On the contrary, at MCP angle 30° and 60° , the difference is less than 0.6 Nm, indicating that those two cases are reasonable results even considering expectable errors mentioned in session 3.2.2.1. The reason for such discrepancy at MCP angle 0° might be mismatch between analysis and experiment condition or other reasons. In order to prove the assumption, it will be discussed in next session.

Table 4-6. Difference between analysis and experiment result according to applied force and MCP angle. (Unit: Nm)

MCP Angle	Applied Force	Analysis (a)	Experiment (b)	Difference (a)-(b)
0°	3kgf	2.606	1.776±0.030	0.832
	4kgf	3.443	2.314±0.022	1.129
	5kgf	4.280	2.705±0.187	1.556
30°	3kgf	2.366	2.077±0.102	0.289
	4kgf	3.130	2.582±0.182	0.548
	5kgf	3.894	3.449±0.211	0.445
60°	3kgf	2.088	1.966±0.068	0.122
	4kgf	2.771	2.705±0.086	0.066
	5kgf	3.455	3.261±0.063	0.194

4.1.4 Discussion

As it is mentioned in previous session, in order to find the reason for the difference (See Table 4-6), consideration on the MCP angle deviation due to the magnitude of applied force will be described and using 3D capture system, the range of its deviation will be measured precisely.

4.1.4.1 MCP Angle Deviation According to Magnitude of Applied Force

As MCP angle increases, the difference (Ⓐ-Ⓑ) decreases considering results about MCP angle. For MCP angle 0° , it is considerably big in comparison with that of other MCP angles while difference is smallest at MCP angle 60° . Then, what makes such a difference? Why the difference is the biggest at MCP angle 0° and smallest at MCP 60° ? To answer those questions, analysis and experiment condition are compared.

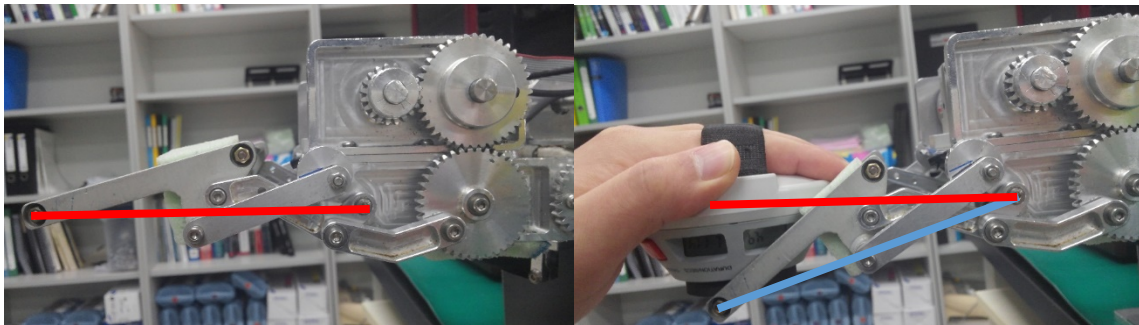


Figure 4-3. Comparison with analysis and experimental condition. Left picture shows before applying force to the hand robot which is analysis condition and right picture shows after applying 5kgf to the hand robot. Red line means reference and blue means the change of link structure after applying 5kgf.

As it is shown in Figure 4-3, after applying force link structure is considerably changed relatively to encoder reading. Seeing with naked eye, MCP angle is changed over 15° while encoder reading is still below 2° . In order to see the angle deviation precisely, 3D motion capture system, VICON, is used.

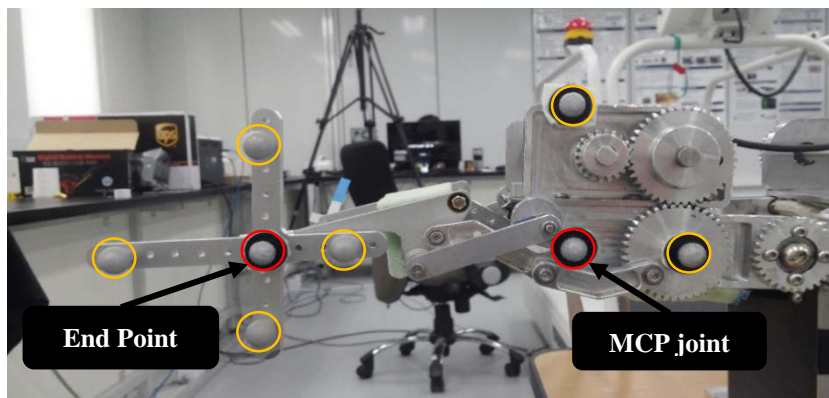


Figure 4-4. Marker setup for tracing the trajectory while applying force to the end-point of the hand robot. 8 markers are attached to end-point, MCP joint, gear, and robot frame. The markers circled as red are interested in this experiment.

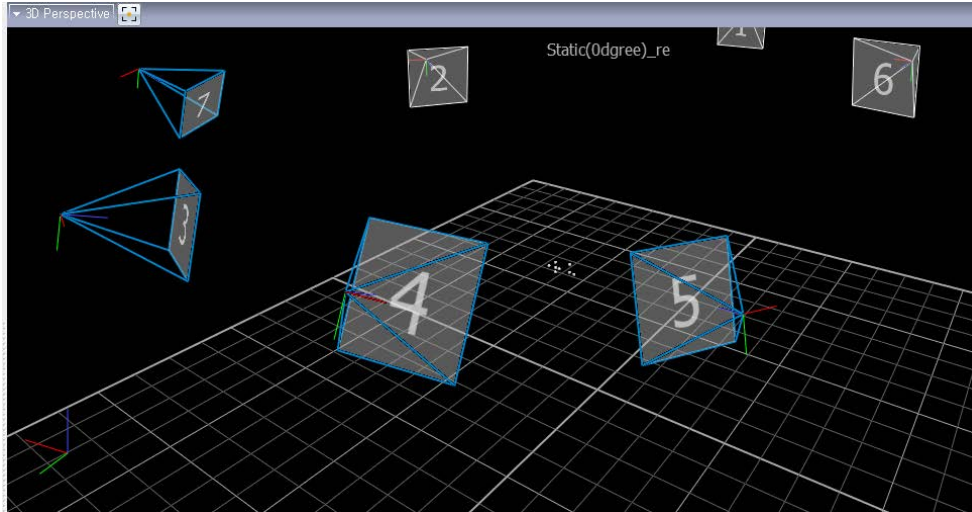


Figure 4-5. VICON camera setup for tracing the markers attached to the hand robot. 4 cameras were used in this experiment. Camera position in 3D space is described for 4 cameras. In the middle of the screen, markers are positioned as a white sphere.

The purpose of this experiment is to measure MCP angle deviation precisely when force is applied to the end-point of the hand robot. Target MCP angles are 0° , 30° , and 60° and applied forces are 3, 4, and 5kgf.

The procedure is progressed as follow. First of all, viewpoint was set by using four Bonita cameras (T-series, VICON). And calibration of each camera is performed by provided software program. As it is shown in Figure 4-5, VICON cameras were set for tracing the markers attached to the hand robot. Four cameras were enough to trace all markers, assuming that all markers are in one plane. For global coordinate configuration, origin was set using wand provided by VICON. Next, markers are attached to the interested points, which are the end-point of the hand robot and MCP joint as shown in Figure 4-4. Then, through NEXUS offered by VICON for data acquisition and data process, the position information of each marker can be obtained, capturing with a velocity of 250frame/sec for about 10 seconds.

Before the estimation of MCP angle deviation, there is assumption that the MCP joint considered as a reference point for this experiment is fixed during the experiment so that y-component is ignored.

Let the position of the end-point of the hand robot express in global coordinate system, (E_x, E_z) and the position of the MCP joint as (P_x, P_z) . Then, distance between two points will be,

$$\overline{EP} = \sqrt{(E_x - P_x)^2 + (E_z - P_z)^2}$$

Also, after moved by applied force, the segment $\overline{E'P}$ must be

$$\overline{E'P} = \sqrt{(E'_x - P_x)^2 + (E'_z - P_z)^2}$$

Of course, a segment $\overline{E'E}$ is estimated by

$$\overline{E'E} = \sqrt{(E'_x - E_x)^2 + (E'_z - E_z)^2}$$

Now, all segments are estimated by simple calculation thus, MCP angle deviation can be calculated by using trigonometric function, second law of cosines. It is given as follow:

$$a^2 = b^2 + c^2 - 2bccosA$$

Where a, b, and c is a segment respectively, A is an angle opposite to side a. From this formula, angle A can be obtained by

$$A = \cos^{-1}\left(\frac{b^2 + c^2 - a^2}{2bc}\right)$$

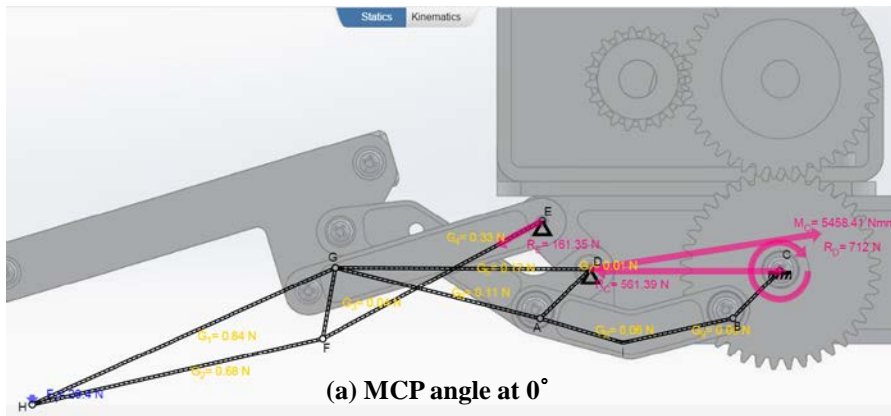
Therefore, the MCP angle deviation, designated by θ_{dev} , can be obtained in this way since all three segments are known. The result of the MCP angle deviation due to applied force is given in Table 4-7 as below.

Table 4-7. MCP angle deviation due to applied force. (Unit: degree)

MCP angle \ Applied force	0°	30°	60°
3kgf	13.5°	8.8°	7.3°
4kgf	16.2°	11.8°	9.5°
5kgf	18.5°	14.8°	10.8°

At all MCP angle, as applied force increases, MCP angle deviation also increases. Also, comparing all three MCP angle cases, the deviation decreases as MCP angle increases. In conclusion, angle deviation due to applied force can explain why the gap exists and it decreases as MCP angle increases, describing that the difference is the maximum at MCP angle 0°. Then, such considerable angle deviation should be included in analysis so that it might diminish the gap.

4.1.5 Results of Modified Analysis of the Hand Robot



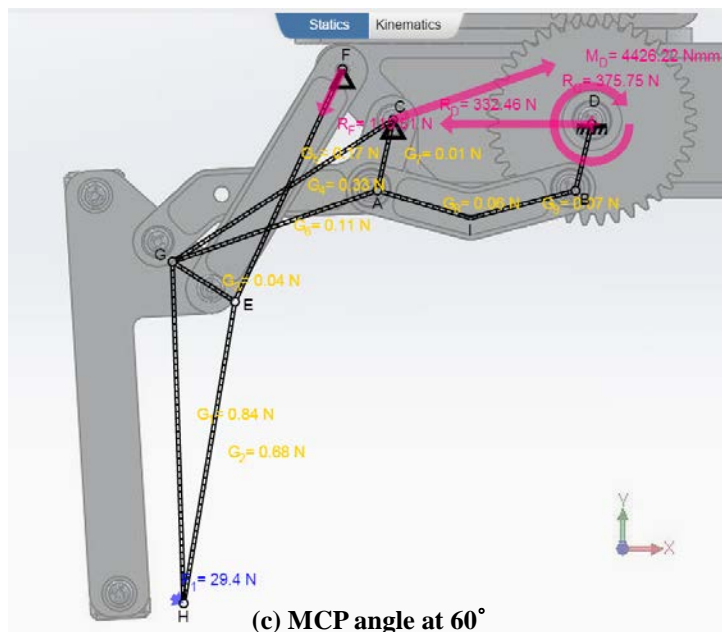
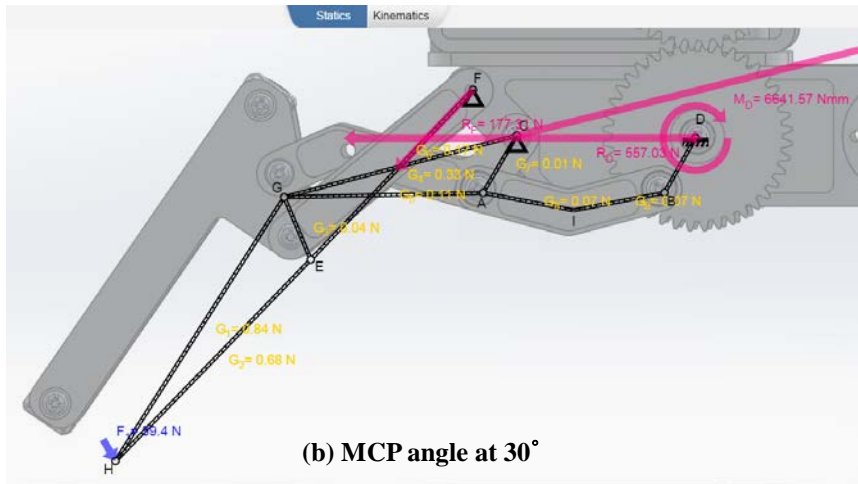


Figure 4-6. Modified link structure according to MCP angle deviation due to applied force. (a) MCP angle at 0° (b) MCP angle at 30° (c) MCP angle at 60°.

Modified link structure according to MCP angle deviation is described in Figure 4-6. As it is clearly seen, the deviation can be figured out obviously throughout all cases. Since MCP angle deviation is different from as applied force increases, it should be considered respectively for each case. Modified analysis results are displayed in Table 4-8 as below. As it is shown in Table 4-8, it is obvious that the difference (a)-(b) considerably decreases compared to previous analysis results. Considering the effect of magnitude and angle deviation of applied force (See 3.3.2), the difference at MCP angle 30° and 60° can be acceptable so that analysis and experiment result at MCP angle 30° are corresponding each other as well as that of MCP angle 60°. Moreover, since it is not general to measure human grip force at MCP angle 0° in contemporary medical field, thus only results of MCP angle 30° and MCP angle 60° are meaningful for this research.

Table 4-8. Modified analysis result according to applied force and MCP angle deviation. (Unit: Nm)

MCP Angle	Applied Force	Modified Analysis Ⓐ	Experiment Ⓑ	Difference Ⓐ-Ⓑ
0°	3kgf	2.405	2.060±0.01	0.345
	4kgf	3.108	2.671±0.01	0.437
	5kgf	3.893	3.382±0.03	0.511
30°	3kgf	2.199	2.125±0.04	0.074
	4kgf	2.831	2.844±0.01	-0.013
	5kgf	3.396	3.359±0.04	0.04
60°	3kgf	1.925	1.970±0.01	-0.045
	4kgf	2.493	2.612±0.03	-0.119
	5kgf	3.086	3.162±0.05	-0.076

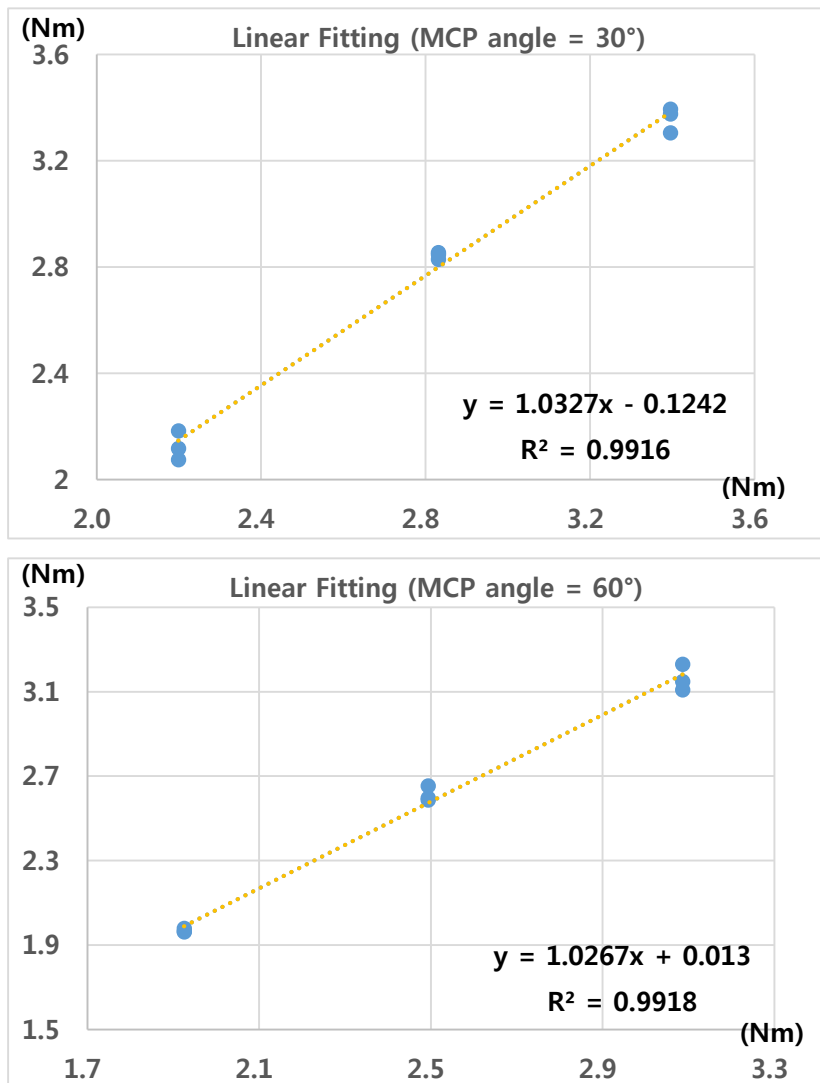


Figure 4-7. Linear fitting with modified analysis results and experiment results. X axis represents analysis result and y axis for experiment result. Among 5 data, maximum and minimum values are extracted so that three experiment results are matched to one analysis result.

To see the relationship between analysis and experiment results clearly, linear fitting with modified analysis results and experiment results are implemented as shown in Figure 4-7. The equations for the relation between modified analysis and experiment results are given as follow.

$$\text{for MCP angle } 30^\circ, \quad y = 1.0327x - 0.1242 \quad \text{with } R^2 = 0.9918$$

$$\text{for MCP angle } 60^\circ, \quad y = 1.0267x + 0.0130 \quad \text{with } R^2 = 0.9916$$

Except for the case of MCP angle 0° , the relation between modified analysis and experiment results shows a high linearity. Therefore, it can be concluded that the relation between torque from F/T sensor and applied force to the end-point of the hand robot is verified and acceptable through experiments and analysis. Finger force can be estimated inversely by that relation. Finally, since torque information from F/T sensor is now validated by this analysis so that the foundation for the impedance control is established.

V. CONCLUSIONS

6.1 Study Summary

The noble hand rehabilitation robot has been developed in author's laboratory for the purpose of providing therapy to stroke patients. There are notable features of the hand robot in terms of mechanism, structures, and training mode. By using plunger the hand robot is capable of adjusting finger holding part for various finger lengths. Considering the survey of measuring adults' finger length, its range is within 44mm to 91mm which demonstrates that our hand robot covers those ranges. Moreover, by using only one actuator, it delivers full grasping motion to subjects.

In terms of training mode, there are two modes for this hand robot: one is passive training mode and the other is active training mode. For passive mode, subject's hand is trained by hand robot with a certain ROM. Of course, ROM can be selective; moreover, training speed also can be accustomed to subject's hand condition and preference. On the other hand, for active mode, a subject can voluntarily move his or her hand without following any defined trajectory. In this mode, impedance control is supposed to be applied but it has not been completed because force information from F/T sensor is not reliable and validated. Thus, in order to implement impedance control to our robot system, the process of verification should be performed for ensuring that force sensed from F/T sensor is reliable data for the realization of impedance control. In other words, relationship between torque at F/T sensor and force applied at the end-point of the hand robot should be explained.

Force analysis of the hand robot is performed using simulation tool, ForceEffect™. First, simplified the hand robot model in 2D plane, and then force from 3kgf to 5kgf is applied one by one at the end-point of the hand robot and plot the output torque of each case while changing MCP angle from 0°, 30°, and 60° to see how the torque is different from MCP angle and the magnitude of applied force. Likewise, simple experiment is performed using digital dynamometer to compare with analysis results.

Finally, the relationship between torque and applied force is identified. And it is clearly manifested that human fingertip force can be estimated from torque sensed at F/T sensor by that relationship. Also, according to previous study result of stroke patients' grip force, it is expected that our hand robot could be feasible for stroke patients. In conclusion, impedance control for the purpose of hand therapy is practicable ensuring that force estimated by the relationship is reliable.

6.2 Limitations

Although the relationship between analysis and experiment results is identified, there are some limitations that remain unsolved during this research. Interestingly, the difference between experiment results and analysis result at MCP angle 0° still remains in comparison with other results at 30° and 60° even though modified analysis result is applied. To conclude, one possible reason is a clearance occurs at joints. In order to figure out such clearance obviously, clearance at each joint is examined one by one. In contrast with other joints, at joint E and joint G in Figure 3-11 clearance is much larger. Moreover, at MCP angle 0° such clearance is presented particularly among all MCP angles. Thus, though modified analysis condition is considered, such a big difference between analysis and experiment results still exists especially at MCP angle 0° .

Another limitation for this research is that mechanism of our hand robot constrains subjects' maximum voluntary grip force (MVGf). Specifically, the bar which subject's hand is lying on is not firm enough to stand when a subject tries to generate maximum grip force as shown in Figure 5-1. It gives a subject pain during generating grip force so that a subject cannot reach the maximum grip force. On the other hand, in contemporary medical field, Jamar dynamometer is widely used for measuring grip force and it has firm base which gives less pain while squeezing hand. Thus, it is required that the bar needs to be more firmly sustainable so that subjects are more likely to generate their maximum grip force.



Figure 5-1. Picture of wearing hand robot

6.3 Future Directions

Through this research, some limitations of our hand robot are described. As it is mentioned in previous chapter, the supporting bar should be modified in order to help subjects generate maximum grip force, thus, design of the bar will be required. After modification, impedance control will be applied to our hand robot. Proper gain tuning of impedance parameters such as mass, damping, and stiffness is required for three different states, high, medium and low impedance, through many trials and errors so that the quality of hand rehabilitation robot therapy will be improved.

Also, the linear equation for all MCP angles will be dealt with. Practically, stroke patients have different contracture and spasticity so that it is hard and cumbersome to position subject's hand to either MCP angle 30° or 60° . Therefore, it is required to have the optimized linear equation that covers all MCP angles, maintaining error small. To obtain the equation, extra experiments will be required.

References

- [1] Palazzolo, J. J., et al. (2007). "Stochastic estimation of arm mechanical impedance during robotic stroke rehabilitation." *IEEE Transactions on Neural Systems and Rehabilitation Engineering*, 15(1), pp. 94-103.
- [2] Teismann, I. K., et al. (2011). "Cortical swallowing processing in early subacute stroke." *BMC Neurol.*, vol.11, 34.
- [3] World Health Organization. Causes of death 2008 summary tables [Internet]. Geneva: World Health Organization [cited 2012 Sep 17]. Available from: http://www.who.int/entity/gho/mortality_burden_disease/
- [4] American Stroke Association, 2005 [Online]. Available: <http://www.strokeassociation.org/>
- [5] Rathore S, Hinn A, Cooper L, Tyroler H, Posamond W. (2002). "Characterization of incident stroke signs and symptoms: findings from the atherosclerosis risk in communities study." *Stroke*, vol. 33, pp. 2718-2721.
- [6] J. Van der Lee, I. Snels, H. Beckerman, G. Lankhorst, R. Wagenaar, and L. Bouter. (2001). "Exercise therapy for arm function in stroke patients: A systematic review of randomized controlled trial." *Clin. Rehabil*, 15(1), pp. 20–31.
- [7] Rochester Hand Center. Bones and Joints Anatomy of Hand. [Internet]. Available from: <http://rochesterhandcenter.com/education.php?article=handanatomy>
- [8] Lance JW. (1980). The Control of Muscle Tone, Reflexes, and Movement: Robert Wartenberg lecture. *Neurology*; 30:1303-1313.
- [9] Kamper DG, Rymer WZ. (2000). "Quantitative features of the stretch response of extrinsic finger muscles in hemiparetic stroke" *Muscle Nerve*. 23(6), pp.954-61.
- [10] Roberts, H. C., et al. (2011). "A review of the measurement of grip strength in clinical and epidemiological studies: towards a standardised approach." *Age and Ageing* 40(4): 423-429.
- [11] Innes E. Handgrip strength testing: a review of the literature. *Aust Occup Ther J* 1999; 46: 120–40.
- [12] Pronk CN, Niesing R. Measuring hand-grip force, using a new application of strain gauges. *Med Biol Eng Comput* 1981; 19(1):127-128.
- [13] Nordenskiöld UM, Grimby G. Grip force in patients with rheumatoid arthritis and fibromyalgia and in healthy subjects. A study with the Grippit instrument. *Scand J Rheumatol* 1993; 22(1):14-19.

- [14] Ashton LA, Myers S. Serial grip strength testing- Its role in assessment of wrist and hand disability. *The Internet Journal of Surgery* 2004; 5(2).
- [15] N. Hogan (1985). "Impedance control: an approach to manipulation," *ASME J.of Dyn., Sys. Meas., and Contr.*, vol. 107, pp. 1–24.
- [16] Innes, E. (1999). "Handgrip strength testing: A review of the literature." *Australian Occupational Therapy Journal* 46(3): 120-140.
- [17] Size Korea. "6th Korea Anthropometric Survey Report", 2010 [Online]. Available from:
<http://sizekorea.kats.go.kr/>
- [18] Koo, Kwang min. "Design of Hand Exoskeleton for Rehabilitation in Stroke", MS, Thesis, Korea Advanced Institute of Science and Technology, Daejeon, Republic of Korea, 2010, 77 pages.
- [19] Boissy, P., et al. (1999). "Maximal grip force in chronic stroke subjects and its relationship to global upper extremity function." *Clinical Rehabilitation*, vol. 13(4), page 354-362.

요 약 문

손 재활로봇의 임피던스 제어를 위한 접지력 측정 검증

최근에 뇌졸중과 같은 신경학적 장애를 가진 사람들의 손 재활을 위한 손 재활로봇이 개발되었다. 메커니즘적인 면에서 볼 때, 이 로봇은 하나의 모터로 파지 운동(full grasping motion)을 할 수 있을 뿐 아니라, 손가락 고정부분을 길이 조절이 가능하게 설계하여 손 길이가 다양한 사람들이 사용할 수 있는 장점을 가졌다. 하지만 앞서 언급한 장점들에도 불구하고, 임피던스 제어를 위해서 필요한 힘/토크센서에서 측정되는 힘에 대한 검증이 이루어지지 않았다. 실제, 임피던스 컨트롤이 적용된 상태에서는 손 재활 운동 중에 손의 직접적인 힘을 알아내야 한다. 따라서, 개발된 손재활로봇에 임피던스 제어를 적용하기 위해서는 손 힘의 신뢰성을 검증할 필요가 있다.

본 논문은 새롭게 개발된 손 재활로봇의 정역학 분석을 통해 로봇 끝 단(end-point)에 가해진 힘과 그로 인해 발생하는 토크 값의 관계를 규명하여 향후 임피던스 제어 구현을 목표로 한다. 이를 위해 먼저, 시뮬레이션 소프트웨어 ForceEffect™를 이용하여 로봇 끝 단에 가해진 힘과 그 때 발생하는 토크 간의 관계를 얻을 수 있었다. 분석 결과를 검증하기 위해 시뮬레이션 조건과 동일한 조건에서 실험을 실시하여 얻은 결과를 분석 결과값과 비교한 결과, 토크 값은 손 MP 관절의 각도와 가하는 힘의 크기와 비례관계를 보임을 알 수 있었다. 그리고, 손 MP 관절이 0도일 경우를 제외한 나머지 30도와 60도에서 분석 결과와 실험 결과 값이 높은 선형성을 보였다. 따라서, 이 선형 방정식을 통해서, 측정되는 토크 값으로부터 사람 손의 힘을 역으로 유추해 낼 수 있고, 손 재활로봇을 이용한 임피던스 제어 구현을 위한 기반을 확립하였다.